Original Article

Diagnostic value of double low-dose targeted perfusion CT imaging for the diagnosis of invasive and preinvasive pulmonary ground-glass nodules: systematic review and meta-analysis

Yu Wu, Bao Chen, Li Su, Xiang Qiu, Xiaoyan Hu, Wenbo Li

Department of Radiology, Chengdu First People's Hospital (Integrated TCM & Western Medicine Hospital Affiliated to Chengdu University of TCM), Chengdu, China

Contributions: (I) Conception and design: Y Wu; (II) Administrative support: W Li; (III) Provision of study materials or patients: B Chen; (IV) Collection and assembly of data: L Su; (V) Data analysis and interpretation: All authors; (VI) Manuscript writing: All authors; (VII) Final approval of manuscript: All authors.

Correspondence to: Wenbo Li. Department of Radiology, Chengdu First People's Hospital (Integrated TCM & Western Medicine Hospital Affiliated to Chengdu University of TCM), Chengdu 610017, China. Email: yost309@163.com.

Background: This study aimed to systematically evaluate and compare the diagnostic value of bubble lucency, interface, lobulated margin and spiculation in distinguishing early invasive and preinvasive intrapulmonary ground-glass nodules (GGNs) using evidence-based meta-analysis methods. Dual low-dose targeted perfusion computed tomography (CT) imaging is controversial in the diagnosis of invasive and preinvasive ground-glass nodules. Different studies have different views and opinions. Therefore, it is necessary to conduct a systematic review of this subject in the form of meta-analysis to guide clinical diagnosis and treatment.

Methods: PubMed, Web of Science, Cochrane library and Embase were searched for recent documentation on the diagnostic value of different signs in invasive and preinvasive pulmonary GGNs. CT imaging signs of bubble lucency, speculation, interface, lobulated margin, and spiculation were used as diagnostic references to discriminate pre-invasive and invasive disease. The sensitivity, specificity, summary receiver operating characteristic (SROC) curves, and the area under the SROC curve (AUC) were calculated to evaluate diagnostic efficiency.

Results: The diagnostic sensitivity and specificity using bubble lucency as a reference of invasive ground-glass opacity (GGO) discrimination was 0.33 (0.24–0.44) and 0.74 (0.62–0.83) respectively. For interface, lobulated margin, and speculation, the diagnostic sensitivity were 0.30 (0.21–0.41), 0.49 (0.39–0.60) and 0.22 (0.14–0.33); and the specificity were 0.83 (0.74–0.89), 0.66 (0.49–0.80) and 0.86 (0.67–0.95). The pooled ROC curve was drawn by sensitivity against 1-specificity using Stata version 15.0. The area under the ROC curve (AUC) values were 0.53, 0.60, 0.58, and 0.43 for bubble lucency, speculation, lobulated margin, and pleural indentation of GGO for discriminating pre-invasive and invasive disease.

Conclusions: The diagnostic value of a single CT imaging sign of GGO, such as bubble lucency, speculation, interface, lobulated margin, and spiculation is limited for discriminating pre-invasive and invasive disease because of low sensitivity, specificity, and AUC.

Keywords: Ground-glass nodules (GGNs); benign and malignant pulmonary ground-glass nodules; invasive lesions; preinvasive lesions

Submitted Feb 26, 2022. Accepted for publication Jul 18, 2022.
doi: 10.21037/tcr-22-790
View this article at: https://dx.doi.org/10.21037/tcr-22-790

Introduction

Lung cancer is a common malignant tumor that seriously affects a patient's survival and quality of life. In recent years, lung squamous cell carcinoma incidence has gradually decreased, while adenocarcinoma incidence has gradually increased to become the most common type of lung cancer (1). Minimally invasive adenocarcinoma (MIA) and invasive adenocarcinoma (IA) are invasive lesions. Multiple studies have shown that the annual 5-year survival rate of preinvasive lesions, i.e., atypical adenomatous hyperplasia (AAH) and adenocarcinoma in situ (AIS) in the new taxonomy, is close to 100% (2). According to their different components, GGNs can be divided into pure ground-glass nodules (pGGNs) and mixed ground-glass nodules (mGGNs). However, any lesion that causes increased density and thickening can be a GGN, so GGNs are a nonspecific sign of intrapulmonary disease. Desai *et al.* (3) reported that 18% of pGGNs and 63% of mGGNs are malignant. A study conducted by Friese-Hamim *et al.* (4) showed that up to 59% of stable pGGNs evolve into AIS or MIA. Another study conducted by Taheri *et al.* (5) showed that approximately 75% of stable GGNs are bronchioloalveolar or adenocarcinomas, which was similar to the findings of the Takada *et al.*'s study (6). The diagnosis of lung cancer is made based on clinical manifestations, fiberoptic bronchoscopy, tumor markers, ordinary X-rays, and computed tomography (CT) examinations (7). However, the symptoms and signs of early lung cancer are not obvious, and most patients are already in the middle and advanced stages at diagnosis. Fiberoptic bronchoscopy and tumor markers are generally used for further examination of patients with suspected lung cancer (8,9). CT perfusion imaging is a new auxiliary examination method, which is different from dynamic scanning. It is a continuous CT scan of the related of interest (ROI) layer during rapid intravenous infusion of contrast agent, so as to obtain the time-density curve of ROI, and calculate the values of various perfusion parameters by using different mathematical models. In recent years, CT perfusion imaging has been gradually applied in lung cancer patients, which plays an important role in the diagnosis, treatment and staging of lung cancer.

In recent years, technological developments have led to the wide use of low-dose CT in early lung cancer screening (10,11), which has resulted in higher detection rates of intrapulmonary nodules, and especially of GGNs. Several imaging features, such as bubble lucency, speculation, interface, lobulated margin, and spiculation, were commonly used to predict pathology type. However, the discrimination power of CT imaging features to discern pre-invasive from invasive lesions is unclear. Therefore, it is necessary to conduct a systematic review of this subject in the form of meta-analysis to guide clinical diagnosis and treatment. We present the following article in accordance with the MOOSE reporting checklist (available at https://tcr.amegroups.com/article/view/10.21037/tcr-22-790/rc).

Methods

Retrieval policy

Two reviewers independently searched PubMed, Web of Science, Cochrane library and Embase for relevant studies. The search terms included: computed tomography, ground-glass nodule, ground-glass opacity, atypical adenomatous hyperplasia, AIS, and MIA. References of the included studies were also screened to locate additional relevant publications.

Inclusion and exclusion criteria

The inclusion criteria were developed according to the inclusion criteria for diagnostic meta-analyses recommended by the Cochrane Collaboration Network in conjunction with the actual situation of the study. These criteria were as follows: (I) the included population were patients diagnosed with lung GGNs of less than 3 cm in diameter using high-resolution CT images; (II) studies related to double low-dose targeted perfusion CT imaging features to predict invasive and pre-invasive disease; (III) the original data could be extracted directly or indirectly.

The exclusion criteria were as follows: (I) literature that was unrelated to this study or contained duplicated data; (II) the diagnosis of invasive and preinvasive pulmonary GGNs was made using the old classification diagnostic terminology, such as bronchioloalveolar carcinoma; (III) literature with a grouping method that was inconsistent with this study; (IV) non-original research, animal experiments, review literature, abstracts, and lectures; (V) the original data could not be extracted.

Screening and data extraction

Two reviewers independently reviewed the full text of each included study. Disagreement was resolved by discussion

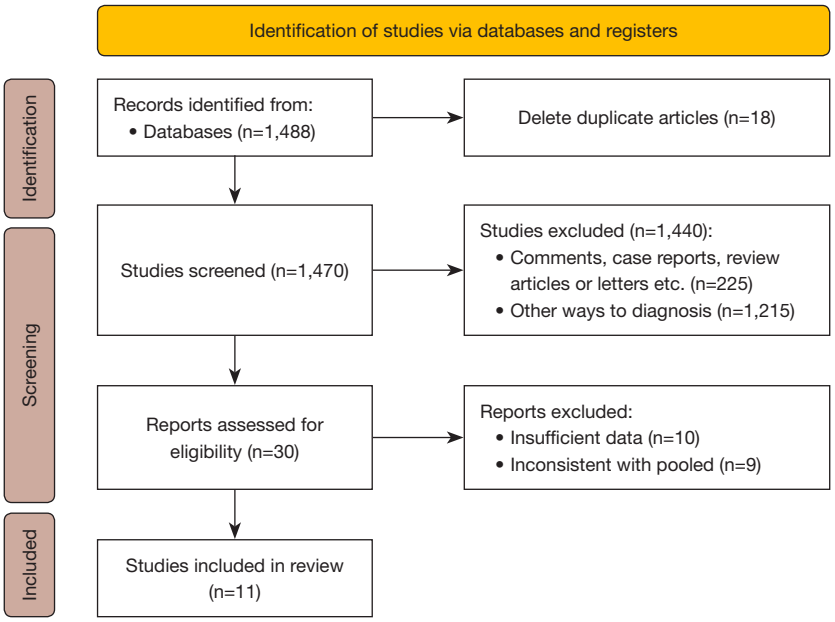

Figure 1 Flow chart of literature retrieval.

or consultation with a third reviewer. The first author names, publication year, the country in which the study was performed. Sex and quantity, lesions located using CT imaging signs of bubble lucency, speculation, lobulated margin, and pleural indentation in pre-invasive and invasive ground-glass opacity (GGO) were also extracted. All data were cross-checked.

Methodological quality assessment of the included studies

The quality of the literature was assessed using the 2011 edition of the Quality Assessment of Diagnostic Accuracy Studies (QUADAS) tool recommended by the Cochrane Collaboration Network. The tool evaluated the following 11 items: participant representativeness, rationality of the gold standard, time interval of the test, partial confirmation bias, different evidence bias, embedded bias, blinded gold standard assessment, blinded diagnostic assessment, clinical information, uncertain results, and loss to follow-up. Each item was evaluated as "yes", "no", or "unclear", with an answer of "yes" receiving 1 point and an answer of "unclear" or "no" receiving 0 points.

Statistical analysis

Diagnostic sensitivity and specificity were calculated using the formulas: sensitivity = true positive/(true positive + false negative); and specificity = true negative/(true negative + false positive). The area under the receiver operating characteristic (ROC) curve was used to evaluate the feasibility of CT imaging features for the diagnosis of pre-invasive and invasive GGO. Publication bias was evaluated using Deek's funnel plot and Egger's line regression test. Two-tailed P values of <0.05 were considered statistically significant. All statistical analysis was performed using Stata version 15.0. I^2<50% and P>0.1 between studies using fixed effect models and I^2>50% and P<0.1 from chi-square analysis showed study heterogeneity. Meta-analysis by random effects models and searched for possible heterogeneity by subgroup analysis source.

Results

Literature search and screening results

A total of 1,488 articles were retrieved, and 18 duplicate articles were excluded after reading the titles and abstracts. A further 123 conference abstracts, 1,215 unrelated studies, 81 reviews, and 21 case reports were excluded. After reading the full text, 19 articles that did not meet the inclusion criteria were excluded. A total of 11 articles (12-22) that met the research criteria were finally included (*Figure 1*).

Table 1 General characteristics of included studies

First author, year	Geographic location	Gender (male/female or total number)	Age (year), mean or mean ± SD
Zhu, 2022 (12)	China	358/660	52.1±10.9
Xiong, 2021 (13)	China	79/121	58.21±10.38
Jiang, 2021 (14)	China	29	55.5
Liu, 2022 (15)	China	70/153	50.3±13.0
Liang, 2015 (16)	China	42/93	59.28±10.14
Yang, 2020 (17)	China	192/449	62.7
Xue, 2018 (18)	China	167/403	58.37±11.40
Zhao, 2019 (19)	China	85/208	54.5±11.8
Meng, 2021 (20)	China	150/359	54
Shi, 2021 (21)	China	114/363	55
Zheng, 2022 (22)	China	103/209	58

Basic features of the included studies

The basic features of the included studies are shown in *Table 1*.

Quality evaluation of the included studies

The 11 included studies (12-22) were of relatively good overall quality (based on QUADAS-2 criteria) in *Figure 2*.

Meta-analysis results

Pooled diagnostic sensitivity and specificity

The diagnostic sensitivity and specificity using bubble lucency as a reference of invasive GGO discrimination was 0.33 (0.24–0.44) and 0.74 (0.62–0.83) respectively. For interface, lobulated margin, and spiculation, the diagnostic sensitivity was 0.30 (0.21–0.41), 0.49 (0.39–0.60) and 0.22 (0.14–0.33); and the specificity was 0.83 (0.74–0.89), 0.66 (0.49–0.80) and 0.86 (0.67–0.95), as shown in *Figure 3*. Therefore, it can be inferred that in this study, we examined the results of previous studies on CT imaging features of GGO, and found that CT imaging features of GGO had low sensitivity and high specificity in distinguishing between preinvasive and invasive lesions.

Pooled receiver operating characteristic curves

The pooled ROC curve was drawn by sensitivity against 1-specificity using Stata version 15.0. The area under the ROC curve (AUC) values were 0.53, 0.60, 0.58, and 0.43 for bubble lucency, speculation, lobulated margin, and pleural indentation of GGO for discriminating pre-invasive and invasive disease. Forest plot of pooled sensitivity and specificity of lesions located using CT imaging signs of bubble lucency, SROC curves of lesions located using CT imaging signs of bubble lucency, interface, lobulated margin and spiculation in pre-invasive and invasive GGO is shown in *Figure 4*.

Publication analysis

Publication bias of GGO features in CT imaging to predict invasiveness was assessed by Deek's funnel plot and Egger's line regression test. No significant bias for bubble lucency (P=0.35), interface (P=0.59), lobulated margin (P=0.38), and spiculation (P=0.41) was observed (*Figure 5*).

Discussion

Adenocarcinoma is a malignant tumor that seriously affects a patient's survival and quality of life (22). Invasive and preinvasive lung GGNs lack specific clinical signs and symptoms in the early stages, and most patients diagnosed with lung cancer are in the middle and advanced stages at the time of treatment (23). Early preinvasive and invasive pulmonary GGNs are adenocarcinomas that are smaller than 3 cm in diameter, with pathological types

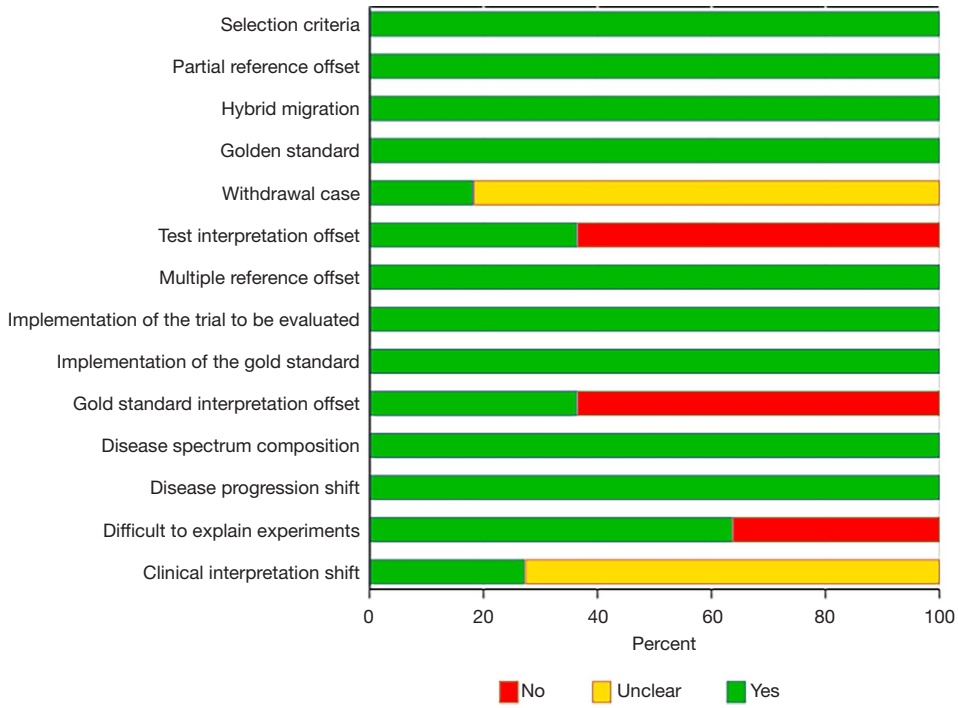

Figure 2 Risk of bias of included studies.

including AAH, AIS, and MIA. Invasive and preinvasive pulmonary nodules predominantly present as GGNs on high-resolution CT images. Histopathology shows that AAH is a proliferative foci of the lungs caused by atypical proliferation of alveolar cells on the alveolar or bronchial wall (24). Because the proliferating tumor cells only cause mild to moderate stenosis of bronchioles and the alveoli have not been completely tamponed by proliferating tumor cells, AAH typically presents as a pure glassy dense nodule. AIS tumor cells grow along the alveolar or bronchial wall. As the number of accumulation layers increases, severe narrowing or even occlusion of the bronchioles can occur, resulting in alveolar collapse. Therefore, some AIS may appear as GGNs on high-resolution CT. With the invasion of tumor cells in the interstitium, blood vessels and traction-adjacent pleura can develop into MIA and IA. Unlike AIS, the solid components in MIA are mostly scar tissue, with only a small amount of alveolar collapse. Most of the solid components in IA are fibroblasts, and only a few are scar tissue or bronchovascular bundle structures (24).

Recent research has focused on the relationship between CT signs of GGNs and different pathological processes. Since the publication of the International Multidisciplinary Classification of Lung Adenocarcinoma in 2011, scholars have conducted extensive research on intrapulmonary GGNs. However, the focus of each study is different, the inclusion criteria for GGNs and the grouping criteria for lesion types are not consistent, the evaluation of nodule imaging signs is subjective Therefore, the objective of this study was to systematically evaluate the quality of previous studies and to analyze the diagnostic value of the size, density, vacuole, burr, lobular, and pleural depression signs in early preinvasive and invasive intrapulmonary GGNs in high quality literature (25). Some studies have investigated other observational indicators, such as lesion volume, quality, and relationship with blood vessels or bronchi, etc. Although these studies reported high differential diagnostic significance, comparability is challenging due to small sample sizes and clinical practices that are difficult to measure, and so a systematic review of these indicators has yet to be carried out.

The cause of this may be that the proportion of AAH included in the preinvasive lesions in this study was higher and the average diameter of the preinvasive lesions was therefore smaller than that of other studies, leading to the other studies displaying better homogeneity. A reason for this could be that the population of this study was European, while that of the other studies was Asian. In addition, the

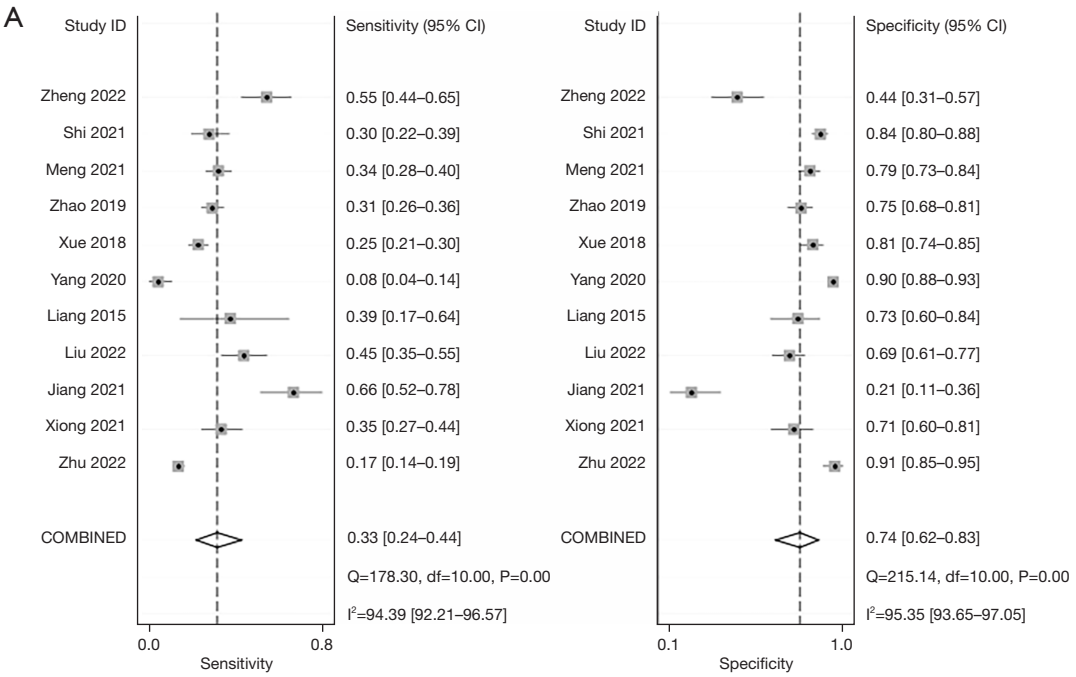

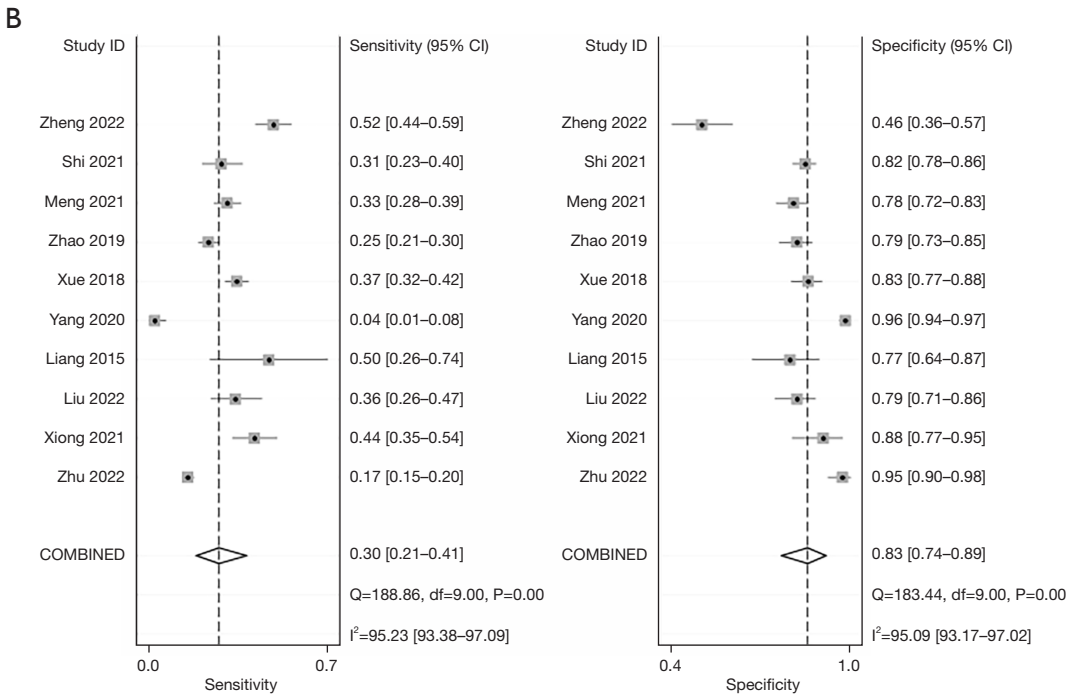

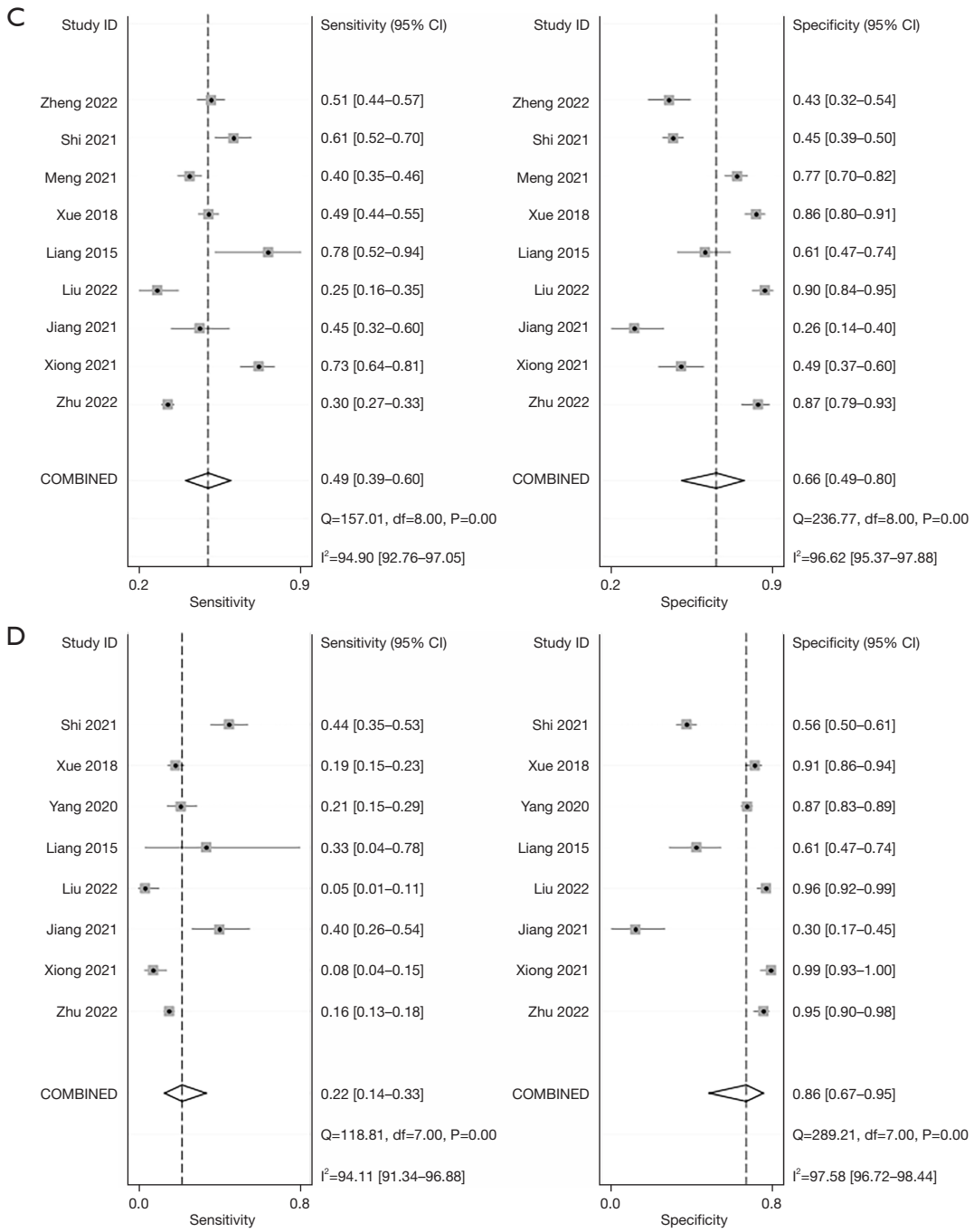

Figure 3 Forest plot of pooled sensitivity and specificity of (A) bubble lucency, (B) interface, (C) lobulated margin and (D) spiculation.

measurement of nodules in different studies was influenced by subjective factors, such as the measurement method and the choice of the maximum measurement cross-section.

In addition, there may be heterogeneity due to other factors, such as inconsistencies in GGN sweep parameters and reconstruction layer thickness between studies, resulting in varying degrees of partial volumetric effects, as studies have shown that the density of nodules is related to the thickness of the reconstructed layer.

The analysis of vacuole, burr, lobular, and pleural

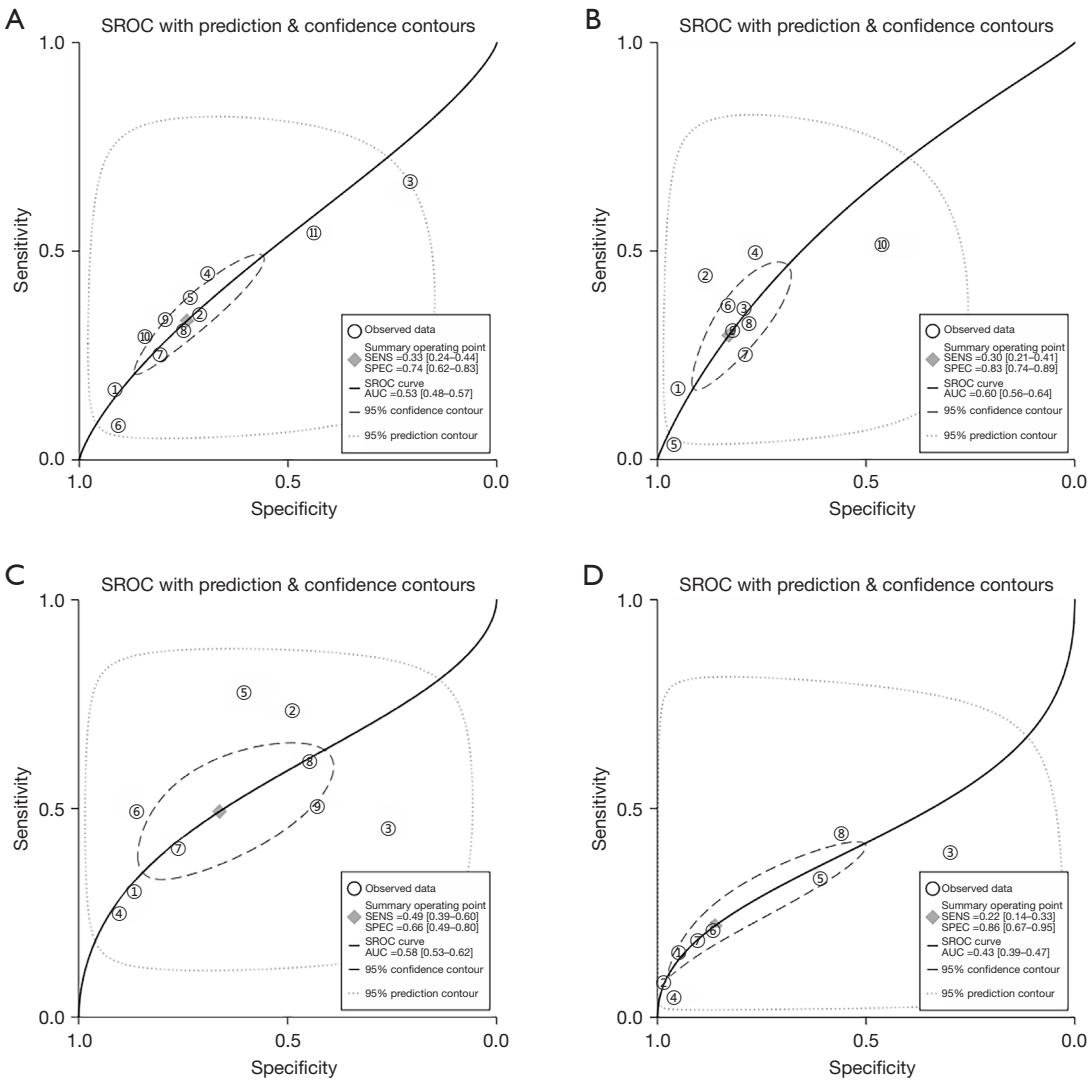

Figure 4 The SROC curves of characteristics including (A) bubble lucency, (B) speculation, (C) lobulated margin and (D) indentation. SROC, summary receiver operating characteristic; AUC, under the ROC curve.

depression signs. Only pGGNs were included in these studies. The results of the meta-analysis showed that there were different degrees of heterogeneity between the studies, with threshold effects responsible for much of this heterogeneity. In other words, as the sensitivity increased, the specificity decreased, and vice versa.

Studies have shown that the sign of the lesion reflects the different degrees of differentiation and growth rate of each part of the tumor. Therefore, understanding the biological behavior of the tumor can help evaluate the nature of the tumor. When the tumor cells grow along the alveolar wall, the surrounding air-containing lung tissue is pressed, causing alveolar or bronchiolar dilation, which to some extent reflects the high differentiation and slow growth rate of the lesion. The burr sign and pleural depression can be triggered by multiple factors. It is generally believed that the burr sign is formed by the spread and growth of tumor cells along the alveoli or lobular septum in all directions, or the proliferation of the surrounding connective tissue stimulated by tumor cells, or the formation of intracellular fibrosis and the contraction and stretching of tumors. Pleural depression may be due to scar contraction caused by collagen fiber hyperplasia in adenocarcinoma tissue, which is formed by pulling the free visceral pleura through the

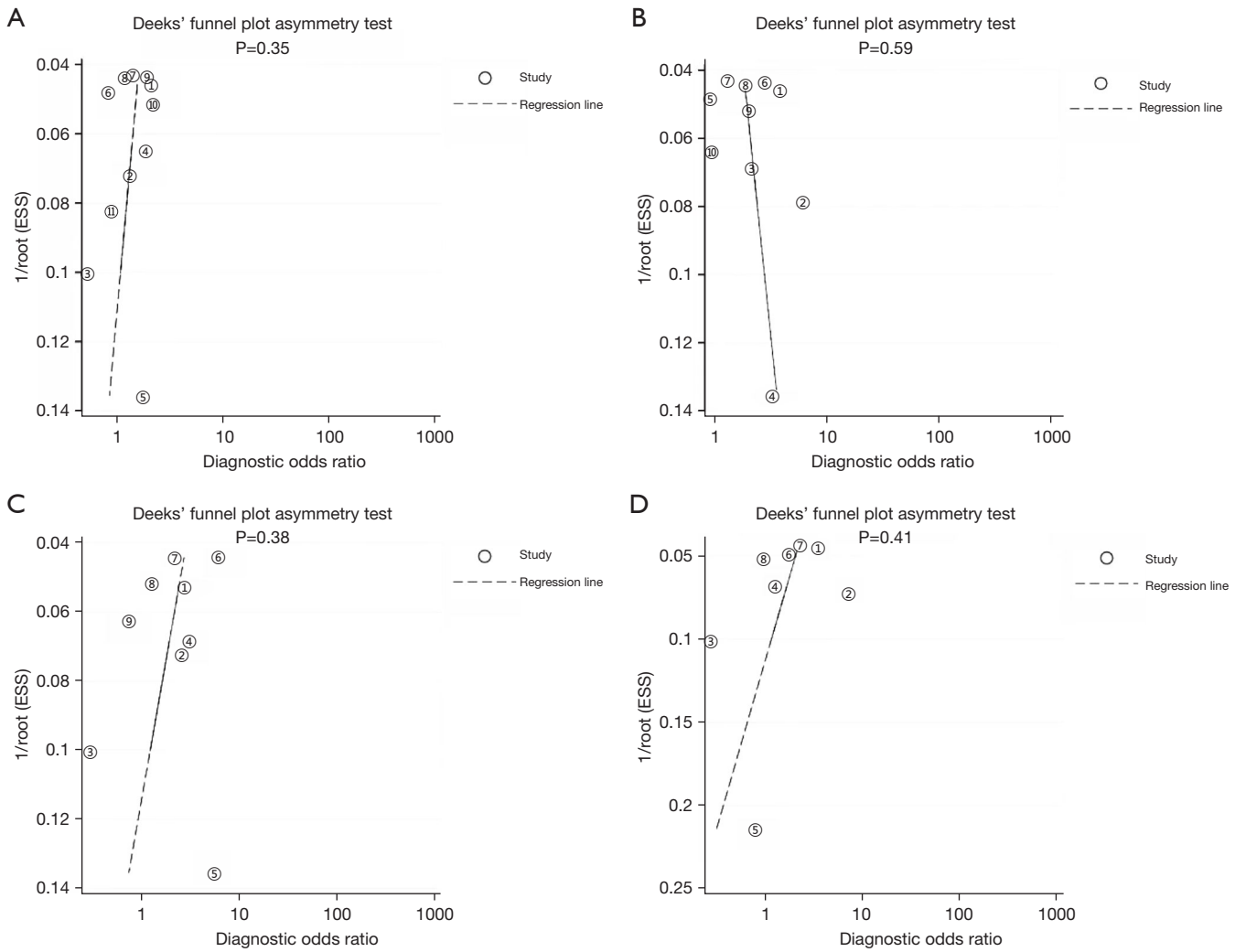

Figure 5 Publication bias evaluated by Deek's funnel plot for computed tomography features: (A) bubble lucency study, and regression line; (B) interface study, and regression line; (C) lobulated margin study, and regression line; (D) spiculation study, and regression line. ESS, Epworth Sleepiness Scale.

fiber scaffold structure of the lung. Therefore, burrs and pleural depression are related to the process of collagen fibrosis in the lesion, and many lesions in the lungs can appear as internal fibrosis. In addition, the occurrence of pleural depression is related to the nodule site; that is, the closer to the visceral pleura, the higher the incidence of pleural depression (26). There are different reports in the literature on the efficacy of burrs and pleural depression signs in the identification of preinvasive and invasive diseases. The results of this study suggested that their diagnostic value for adenocarcinoma is not high, and this is consistent with the results of this study.

Meta-analysis is an evidence-based quantitative method for the systematic analysis and quantitative synthesis of multiple research results with the same purpose, which can effectively increase the sample size of the study, reduce random error, and improve the efficiency of test statistics. Nonetheless, the present study had a number of limitations. First, some imaging studies of GGN contain indicators such as volume, mass, two-dimensional ratio, and three-dimensional ratio in addition to the above imaging signs, but due to the small quantity of literature after screening, a meta-analysis of these indicators could not be performed. Second, although there have been many studies on invasive and preinvasive pulmonary GGNs, the classification and grouping standards of nodules by size and composition in

the included studies was inconsistent. Third, the included studies were mostly from Asia, so it was not possible to conduct an analysis of multi-ethnic populations. Fourth, this study included only Chinese and English research and did not contain unpublished literature, so publication bias could not be excluded. Fifth, subgroup and meta-regression analyses were not performed for heterogeneous sources because of the small number of original studies included. Sixth, meta-analysis is a secondary analysis of existing data, and publication bias may occur in the process, which is an inherent limitation of meta-analysis.

Conclusions

The diagnostic value of a CT imaging of GGO, such as bubble lucency, speculation, lobulated margin, or pleural indentation bubble lucency, interface, lobulated margin and spiculation is limited for discriminating pre-invasive and invasive disease because of low sensitivity and AUC but have high specificity.

Acknowledgments

Funding: The study was supported by the Scientific Research Project of Chengdu First People's Hospital (Chengdu Hospital of Integrated Traditional Chinese and Western Medicine) (No. 2021018).

Footnote

Reporting Checklist: The authors have completed the MOOSE reporting checklist. Available at https://tcr.amegroups.com/article/view/10.21037/tcr-22-790/rc

Conflicts of Interest: All authors have completed the ICMJE uniform disclosure form (available at https://tcr.amegroups.com/article/view/10.21037/tcr-22-790/coif). The authors have no conflicts of interest to declare.

Ethical Statement: The authors are accountable for all aspects of the work in ensuring that questions related to the accuracy or integrity of any part of the work are appropriately investigated and resolved.

References

1. Yang L, Wu D, Chen J, et al. Corrigendum to: A functional CNVR_3425.1 damping lincRNA FENDRR increases lifetime risk of lung cancer and COPD in Chinese. Carcinogenesis 2021;42:1506-7.
2. Hutchinson BD, Shroff GS, Truong MT, et al. Spectrum of Lung Adenocarcinoma. Semin Ultrasound CT MR 2019;40:255-64.
3. Desai A, Abdayem P, Adjei AA, et al. Antibody-drug conjugates: A promising novel therapeutic approach in lung cancer. Lung Cancer 2022;163:96-106.
4. Friese-Hamim M, Clark A, Perrin D, et al. Brain penetration and efficacy of tepotinib in orthotopic patient-derived xenograft models of MET-driven non-small cell lung cancer brain metastases. Lung Cancer 2022;163:77-86.
5. Taheri N, Khoshsafar H, Ghanei M, et al. Dual-template rectangular nanotube molecularly imprinted polypyrrole for label-free impedimetric sensing of AFP and CEA as lung cancer biomarkers. Talanta 2022;239:123146.
6. Takada K, Takamori S, Shimokawa M, et al. Assessment of the albumin-bilirubin grade as a prognostic factor in patients with non-small-cell lung cancer receiving anti-PD-1-based therapy. ESMO Open 2021. [Epub ahead of print]. doi: 10.1016/j.esmoop.2021.100348.
7. Li L, Tang S, Yin JC, et al. Comprehensive next-generation sequencing reveals novel predictive biomarkers of recurrence and thoracic toxicity risks following chemoradiotherapy in limited stage small-cell lung cancer. Int J Radiat Oncol Biol Phys 2021. [Epub ahead of print]. doi: 10.1016/j.ijrobp.2021.12.009.
8. Pan J, Xue Y, Li S, et al. PM2.5 induces the distant metastasis of lung adenocarcinoma via promoting the stem cell properties of cancer cells. Environ Pollut 2022;296:118718.
9. Shefer NA, Topolnitskiy EB, Dambayev GT. Results and features of surgical treatment of lung cancer after previous COVID-19 pneumonia. Khirurgiia (Mosk) 2021;(12):15-9.
10. Influence of genetic variants of opioid-related genes on opioid-induced adverse effects in patients with lung cancer: A STROBE-compliant observational study: Erratum.

Medicine (Baltimore) 2021;100:e28405.
11. Houston T. Screening for Lung Cancer. Med Clin North Am 2020;104:1037-50.
12. Zhu M, Yang Z, Wang M, et al. A computerized tomography-based radiomic model for assessing the invasiveness of lung adenocarcinoma manifesting as ground-glass opacity nodules. Respir Res 2022;23:96.
13. Xiong Z, Jiang Y, Che S, et al. Use of CT radiomics to differentiate minimally invasive adenocarcinomas and invasive adenocarcinomas presenting as pure ground-glass nodules larger than 10 mm. Eur J Radiol 2021;141:109772.
14. Jiang Y, Che S, Ma S, et al. Radiomic signature based on CT imaging to distinguish invasive adenocarcinoma from minimally invasive adenocarcinoma in pure ground-glass nodules with pleural contact. Cancer Imaging 2021;21:1.
15. Liu J, Yang X, Li Y, et al. Development and validation of qualitative and quantitative models to predict invasiveness of lung adenocarcinomas manifesting as pure ground-glass nodules based on low-dose computed tomography during lung cancer screening. Quant Imaging Med Surg 2022;12:2917-31.
16. Liang J, Xu XQ, Xu H, et al. Using the CT features to differentiate invasive pulmonary adenocarcinoma from pre-invasive lesion appearing as pure or mixed ground-glass nodules. Br J Radiol 2015;88:20140811.
17. Yang HH, Lv YL, Fan XH, et al. Factors distinguishing invasive from pre-invasive adenocarcinoma presenting as pure ground glass pulmonary nodules. Radiat Oncol 2020;15:186.
18. Xue X, Yang Y, Huang Q, et al. Use of a Radiomics Model to Predict Tumor Invasiveness of Pulmonary Adenocarcinomas Appearing as Pulmonary Ground-Glass Nodules. Biomed Res Int 2018;2018:6803971.
19. Zhao W, Xu Y, Yang Z, et al. Development and validation of a radiomics nomogram for identifying invasiveness of pulmonary adenocarcinomas appearing as subcentimeter ground-glass opacity nodules. Eur J Radiol 2019;112:161-8.
20. Meng F, Guo Y, Li M, et al. Radiomics nomogram: A noninvasive tool for preoperative evaluation of the invasiveness of pulmonary adenocarcinomas manifesting as ground-glass nodules. Transl Oncol 2021;14:100936.
21. Shi L, Shi W, Peng X, et al. Development and Validation a Nomogram Incorporating CT Radiomics Signatures and Radiological Features for Differentiating Invasive Adenocarcinoma From Adenocarcinoma In Situ and Minimally Invasive Adenocarcinoma Presenting as Ground-Glass Nodules Measuring 5-10mm in Diameter. Front Oncol 2021;11:618677.
22. Zheng H, Zhang H, Wang S, et al. Invasive Prediction of Ground Glass Nodule Based on Clinical Characteristics and Radiomics Feature. Front Genet 2022;12:783391.
23. Cheng Y, Wang Q, Li K, et al. Anlotinib for patients with small cell lung cancer and baseline liver metastases: A post hoc analysis of the ALTER 1202 trial. Cancer Med 2022;11:1081-7.
24. Heynemann S, Mitchell P. Developments in systemic therapies for the management of lung cancer. Intern Med J 2021;51:2012-20.
25. Festari MF, da Costa V, Rodríguez-Zraquia SA, et al. The tumour-associated Tn antigen fosters lung metastasis and recruitment of regulatory T cells in triple negative breast cancer. Glycobiology 2021. [Epub ahead of print]. doi: 10.1093/glycob/cwab123.
26. Cheng N, Cui X, Chen C, et al. Exploration of Lung Cancer-Related Genetic Factors via Mendelian Randomization Method Based on Genomic and Transcriptomic Summarized Data. Front Cell Dev Biol 2021;9:800756.

(English Language Editor: C. Gourlay)

Cite this article as: Wu Y, Chen B, Su L, Qiu X, Hu X, Li W. Diagnostic value of double low-dose targeted perfusion CT imaging for the diagnosis of invasive and preinvasive pulmonary ground-glass nodules: systematic review and meta-analysis. Transl Cancer Res 2022;11(8):2823-2833. doi: 10.21037/tcr-22-790

